

## Supporting Information

### **Synergizing NiOOH Formation and Proton Conduction via Oxygen Vacancy-Induced Dual Regulation for 1,5-Glutaric Acid Synthesis**

*Hao Chen, Zhixiang Yuan, Xinyu Sheng, Shihao Wang, Jun Hu, Ping Chen\**

School of Materials Science and Engineering, Anhui University, Hefei, 230601, P. R. China

Email: chenping@ahu.edu.cn

## **Table of Contents**

**Supplementary Methods**

**Supplementary Fig. 1-8**

## Supplementary Methods

### Experimental Section

#### Chemicals

Nickel (II) nitrate hexahydrate ( $\text{Ni}(\text{NO}_3)_2 \cdot 6\text{H}_2\text{O}$ ,  $\geq 98\%$ ), potassium hydroxide (KOH,  $\geq 85\%$ ), N, N-Dimethylformamide (DMF,  $\text{C}_3\text{H}_7\text{NO}$ ,  $\geq 99.5\%$ ), Sodium borohydride ( $\text{NaBH}_4$ ,  $\geq 98\%$ ), ethanol ( $\text{CH}_3\text{CH}_2\text{OH}$ ,  $\geq 99.7\%$ ), sulfuric acid ( $\text{H}_2\text{SO}_4$ , 95~98%) and acetone ( $\text{C}_3\text{H}_6\text{O}$ ,  $\geq 99.5\%$ ), were purchased from Sinopharm reagent Co., Ltd. Polyvinylpyrrolidone (PVP, K30), ammonium ceric nitrate ( $(\text{NH}_4)_2\text{Ce}(\text{NO}_3)_6$ ,  $\geq 99\%$ ), 1,5-pentanediol ( $\text{C}_5\text{H}_{12}\text{O}_2$ , 97%), and glutaric acid ( $\text{C}_5\text{H}_8\text{O}_4$ , 99%) were purchased from Macklin Biochemical Co., Ltd. All of these reagents were of analytical grade, and directly used without further purification. Deionized (DI) water was used in all experiments ( $18.25 \text{ M}\Omega \cdot \text{cm}$ ).

#### Preparation

**Preparation of  $\text{CeO}_2\text{-Ni}(\text{OH})_2$  on nickel foam.** Nickel foam (NF) was ultrasonically cleaned for 10 minutes each in anhydrous ethanol, deionized water, and 3.0 M hydrochloric acid, followed by thorough rinsing with deionized water and drying in a vacuum oven at 60 °C. 1.5 mmol  $\text{Ni}(\text{NO}_3)_2 \cdot 6\text{H}_2\text{O}$ , 0.2 g PVP, and 1.5 mmol  $(\text{NH}_4)_2\text{Ce}(\text{NO}_3)_6$  were dissolved in a mixed solvent of 30 mL  $\text{H}_2\text{O}$  and 30 mL N,N-dimethylformamide (DMF). The mixture was ultrasonicated at room temperature for 20 min to obtain a homogeneous solution. The resulting solution was then transferred into a 100 mL Teflon-lined autoclave containing a piece of cleaned nickel foam. The autoclave was maintained at 160 °C for 9 h. After naturally cooling to room temperature, the nickel foam was removed from the autoclave, washed alternately with

deionized water and absolute ethanol several times, and finally dried overnight in a vacuum oven at 60 °C.

**Preparation of  $V\theta$ -CeO<sub>2</sub>-Ni(OH)<sub>2</sub> on nickel foam.** 0.12 g NaBH<sub>4</sub> was dissolved in a mixed solution of 10 mL H<sub>2</sub>O and 10 mL ethanol. The mixture was ultrasonicated at room temperature for 5 min to obtain a homogeneous solution, during which 20 mL H<sub>2</sub>O was added dropwise under continuous ultrasonication. The resulting solution was then transferred into a 100 mL Teflon-lined autoclave containing the as-prepared CeO<sub>2</sub>-Ni(OH)<sub>2</sub> catalyst grown on nickel foam. The autoclave was maintained at 120 °C for 8 h. After naturally cooling to room temperature, the nickel foam was removed from the autoclave, washed alternately with deionized water and absolute ethanol three times, and finally dried overnight in a vacuum oven at 60 °C.

### **Characterization**

Transmission electron microscopy (TEM) images were obtained using a JEM-F200 instrument (JEOL Ltd., Japan). X-ray diffraction (XRD) measurements were carried out on a SmartLab 9KW high-resolution diffractometer (Rigaku Corp., Tokyo, Japan) employing Cu K $\alpha$  radiation. Data were collected across a  $2\theta$  range of 5° to 90° with a scanning speed of 10° min<sup>-1</sup>. Scanning electron microscopy (SEM) was performed with an S-4800 microscope (Hitachi Ltd., Japan) operated at an accelerating voltage of 3 kV. X-ray photoelectron spectroscopy (XPS) analyses were conducted on an ESCALAB 250Xi spectrometer (Thermo Fisher Scientific, Waltham, MA, USA). The binding energy scale was calibrated by setting the C1s signal to 284.8 eV. Fourier-transform infrared (FT-IR) spectra were recorded using an iS50 spectrometer (Thermo Fisher

Scientific, Waltham, MA, USA) with samples prepared as KBr pellets. X-ray absorption fine structure (XAS) measurements were performed on a TableXAFS-500 benchtop spectrometer (Speccreation Instruments Co., Ltd., China).

### **Electrochemical measurements**

The electrocatalytic oxidation of 1,5-pentanediol (POR) was investigated in an H-type electrochemical cell at room temperature using a conventional three-electrode setup controlled by an IM6e electrochemical workstation (Zahner-Elektrik, Germany). All potentials were referenced to the reversible hydrogen electrode (RHE) using the conversion equation:  $E_{\text{RHE}} = E_{\text{Hg/HgO}} + 0.098 + 0.0591 \times \text{pH}$ . The electrocatalytic performance was evaluated by linear sweep voltammetry (LSV), electrochemical impedance spectroscopy (EIS), and chronopotentiometry (CP). The electrolyte consisted of 1.0 M KOH with and without 300 mM 1,5-pentanediol. Linear sweep voltammetry was conducted at a scan rate of 5 mV S<sup>-1</sup>; all reported potentials were subjected to 90% iR correction and subsequently converted to the RHE scale. Cyclic voltammetry (CV) was employed to determine the double-layer capacitance ( $C_{\text{dl}}$ ) of the samples within a non-Faradaic potential window (0.1-0.15 V vs. Hg/HgO) at varying scan rates.

### ***In situ* spectroscopy measurement**

***In situ* Raman spectroscopy measurement.** Raman spectroscopy was conducted using a Renishaw inVia confocal Raman microscope equipped with a 532 nm laser excitation source. Electrochemical Raman measurements were carried out under controlled potential conditions to probe the POR process, with applied potentials

ranging from the open circuit potential (OCP) to 1.5 V vs. RHE. A self-supported  $\text{VO}$ - $\text{CeO}_2$ - $\text{Ni}(\text{OH})_2$  electrode served as the working electrode, while an Ag/AgCl electrode and a Pt wire were used as the reference and counter electrodes, respectively.

***In situ ATR-FTIR measurement.*** In situ electrochemical infrared absorption spectroscopy was performed using a PerkinElmer Spectrum 3 spectrometer equipped with a liquid-nitrogen-cooled mercury cadmium telluride (MCT) detector. A catalyst ink was prepared by dispersing 5.0 mg of the catalyst and 10  $\mu\text{L}$  of Nafion solution (5 wt.%) in 590  $\mu\text{L}$  of isopropanol, followed by sonication for 30 minutes to ensure homogeneity. Subsequently, 10  $\mu\text{L}$  of the well-dispersed ink was drop-cast onto Au-coated silicon crystals and allowed to dry naturally under ambient conditions. *In situ* infrared absorption spectra were collected in a 1.0 M KOH electrolyte containing 300 mM 1,5-pentanediol using a standard three-electrode configuration. The as-prepared catalyst, a Pt mesh (1 x 1 cm), and a Hg/HgO electrode served as the working, counter, and reference electrodes, respectively. Spectra were recorded over a potential range from OCP to 0.6 V (vs. Hg/HgO) in 0.1 V increments.

**Spectroscopic analysis of water configurations via Gaussian fitting.** The O-H stretching vibrational region was deconvoluted via Gaussian fitting in Origin software, to resolve spectroscopically distinct hydrogen bonding states. The detailed analytical protocol was as follows: (1) Prior to spectral deconvolution, baseline correction was performed on all as-collected raw spectra to eliminate systematic baseline drift originating from instrumental instability over the measurement period. (2) A multi-Gaussian peak fitting model was adopted to resolve and deconvolute the individual spectral contributions corresponding to each hydrogen-bonded water vibrational mode. The initial center position of each Gaussian component was determined based on previously reported literature values, followed by iterative optimization during the

fitting process to minimize the residual sum of squares and ensure optimal convergence. (3) The relative abundance of distinct interfacial water configurations (e.g., O-down oriented H<sub>2</sub>O molecules) was determined via quantitative integration of the fitted peak areas. The reliability and robustness of this analytical method were verified by fitting uncertainty parameters: the standard deviation of the chi-squared ( $\chi^2$ ) value was maintained below  $10^{-3}$ , with a sum of squares (SS) error of less than  $1.01 \times 10^{-1}$  for all fitting results.

**The kinetic isotope effect (KIE) measurements.** KIE measurements were conducted in a standard three-electrode system. Two 50 mL standard three-electrode electrochemical cells were used, with each containing 30 mL of electrolyte. One electrolyte was a 0.1 M NaOH aqueous solution containing 0.03 M 1,5-pentanediol (H<sub>2</sub>O system), while the other was a 0.1 M NaOD heavy water solution containing 0.03 M 1,5-pentanediol (D<sub>2</sub>O system). A carbon rod was used as the counter electrode, and the differently activated catalytic materials were employed as working electrodes and immersed into the two solutions, respectively. The electrocatalytic activity was evaluated by linear sweep voltammetry (LSV) with a potential scan range of 0 to 0.8 V (vs. Hg/HgO) at a scan rate of 5 mVs<sup>-1</sup>. The KIE value for each catalyst was defined as the ratio of the current density measured in the H<sub>2</sub>O system to that measured in the D<sub>2</sub>O system at the same applied potential (i.e.,  $j_{\text{H}_2\text{O}} / j_{\text{D}_2\text{O}}$ ).

#### **Measurement of 1,5-PDO reactant and ionic product content**

For the quantification of residual 1,5-pentanediol (1,5-PDO), 0.2 mL of the electrolyte was extracted with 2 mL of ethyl acetate following each chronoamperometry test. The resulting organic phase was analyzed using a CEAULIGHT GC-7920 gas chromatograph (GC) equipped with both a thermal conductivity detector (TCD) and a

flame ionization detector (FID). The injector temperature was maintained at 250 °C, and nitrogen was used as the carrier gas at a flow rate of 1.5 mL min<sup>-1</sup>. Ionic products, including GA-K, and HCOOK, were quantified using an IC6210 ion chromatograph (IC, Wayeal AS2800, China) fitted with an anion-exchange column (Wayeal HS-5A-P3, 4.0 x 250 mm) to improve separation efficiency. Prior to analysis, all samples and calibration standards were diluted to a final volume of 0.5 mL using a 500 mL volumetric flask to ensure precise volume control. To guarantee data reliability, each measurement was performed in triplicate, and the average value was reported. The Faraday efficiency (FE) for GA was calculated using the following equations:

$$FE (\%) = \frac{\text{mol of formed 1,5 - GA}}{\text{total passed charge} / (8 \times F)} \times 100\% \quad (1)$$

$$1,5 - GA \text{ yield} (\%) = \frac{\text{mol of formed 1,5 - GA}}{\text{mol of initial 1,5 - PDO}} \times 100\% \quad (2)$$

where n represents the electron transfer number involved in the formation of each product: for 1,5-GA, n= 8; for HCOOH, n = 2; F denotes the Faraday constant (96485 C mol<sup>-1</sup>).

### **Post-reaction workup and product purification**

Upon completion of the POR reaction (2 L of 1,5-pentanediol), 1 L of sulfuric acid solution (1.2 mol L<sup>-1</sup>) was introduced dropwise under continuous stirring to adjust the pH to approximately 2.0. The resulting mixture was then concentrated via vacuum rotary evaporation at 60 °C to yield a solid residue. This solid was repeatedly washed and filtered with anhydrous acetone, with all acetone filtrates being collected. The combined filtrates were further concentrated by vacuum rotary evaporation at 40 °C to obtain a solid product. The resulting solid was purified through additional washing and

filtration with anhydrous acetone, and this process was repeated several times. Finally, the acetone filtrates were evaporated under vacuum at 40 °C to afford a purified solid powder, which was gathered for subsequent qualitative and quantitative analysis.

### **Membrane Electrode Assembly (MEA) reactor**

MEA measurements,  $V_{O}$ -CeO<sub>2</sub>-Ni(OH)<sub>2</sub> (4.0 cm<sup>2</sup>) and Pt/Ti fiber felt (4.0 cm<sup>2</sup>) served as the anode and cathode, respectively. The anolyte consisted of 1.0 M KOH containing 300 mM 1,5-pentanediol, while the catholyte was 1.0 M KOH. A FAA-3-PK130 membrane (Fumasep) was employed as the separator. Electrolyte circulation was driven by peristaltic pumps. The cell stability of the MEA for POR was evaluated through chronoamperometry at 2 A for 15 consecutive cycles, each lasting 12 h. All electrochemical measurements were conducted under ambient conditions.

## Supplementary Figures

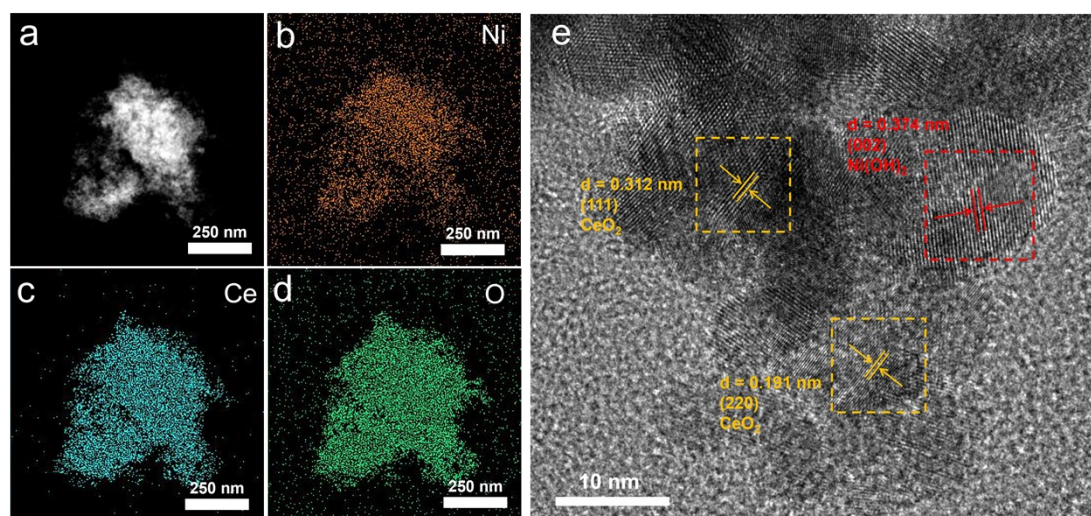


**Fig. S1** TEM image of  $V_o$ - $CeO_2$ - $Ni(OH)_2$ , elemental mapping of the corresponding area: Ni (b), Ce (c), and O (d). (e) High-resolution TEM of  $V_o$ - $CeO_2$ - $Ni(OH)_2$ . The yellow dashed boxes highlight lattice fringes with spacings of 0.312 nm and 0.191 nm, corresponding to the (111) and (220) planes of  $CeO_2$ , respectively. The red dashed box reveals lattice fringes with a spacing of 0.374 nm, indexed to the (002) plane of  $Ni(OH)_2$ .

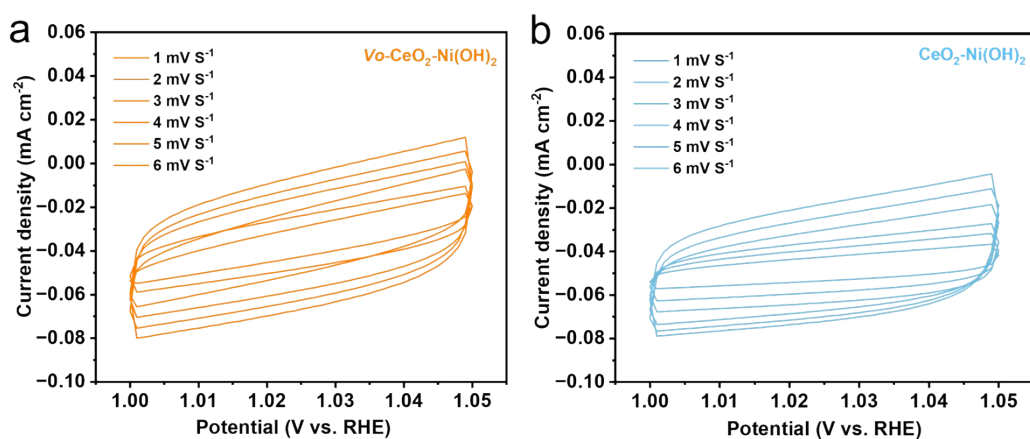


**Fig. S2** (a) Cyclic voltammetry (CV) curves of  $V_o$ - $CeO_2$ - $Ni(OH)_2$  and (b)  $CeO_2$ - $Ni(OH)_2$  in the non-faradaic region (1.00-1.05 V vs. RHE) at different scan rates (1-6  $mV s^{-1}$ ).

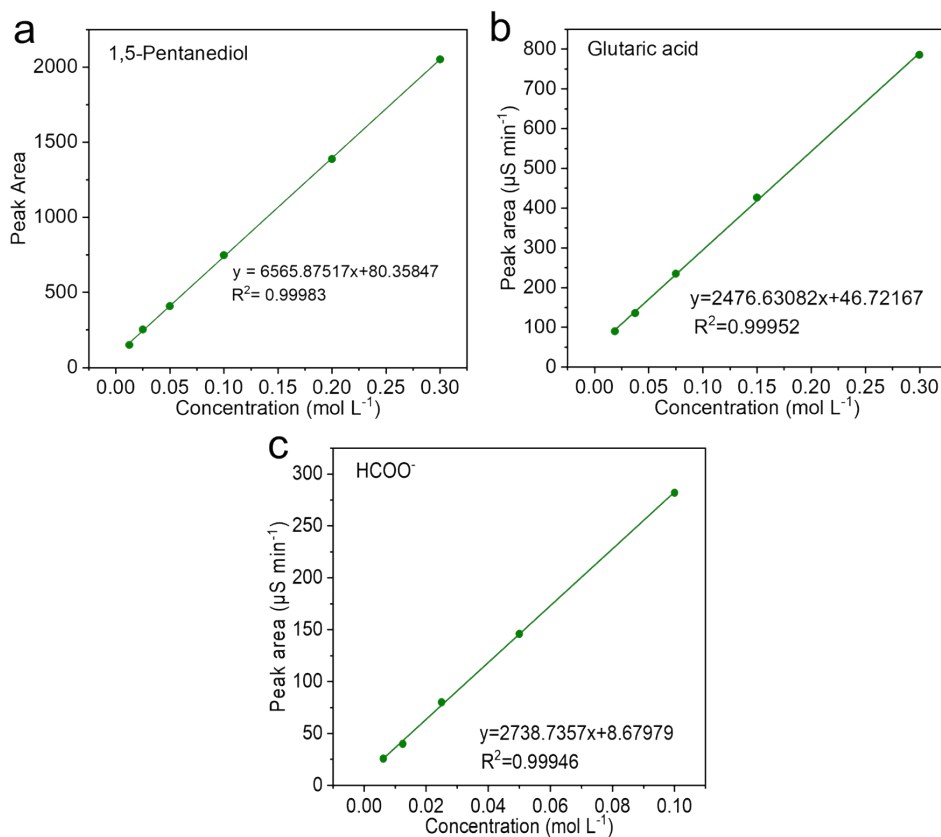


**Fig. S3** Standard calibration curves for quantitative analysis of products and substrates: (a) Gas chromatography (GC) calibration curve for 1,5-PDO; (b-d) Ion chromatography (IC) calibration curves for (b) 1,5-GA, (c) HCOOH. The corresponding linear fitting equations and correlation coefficients ( $R^2$ ) are shown in the figure.

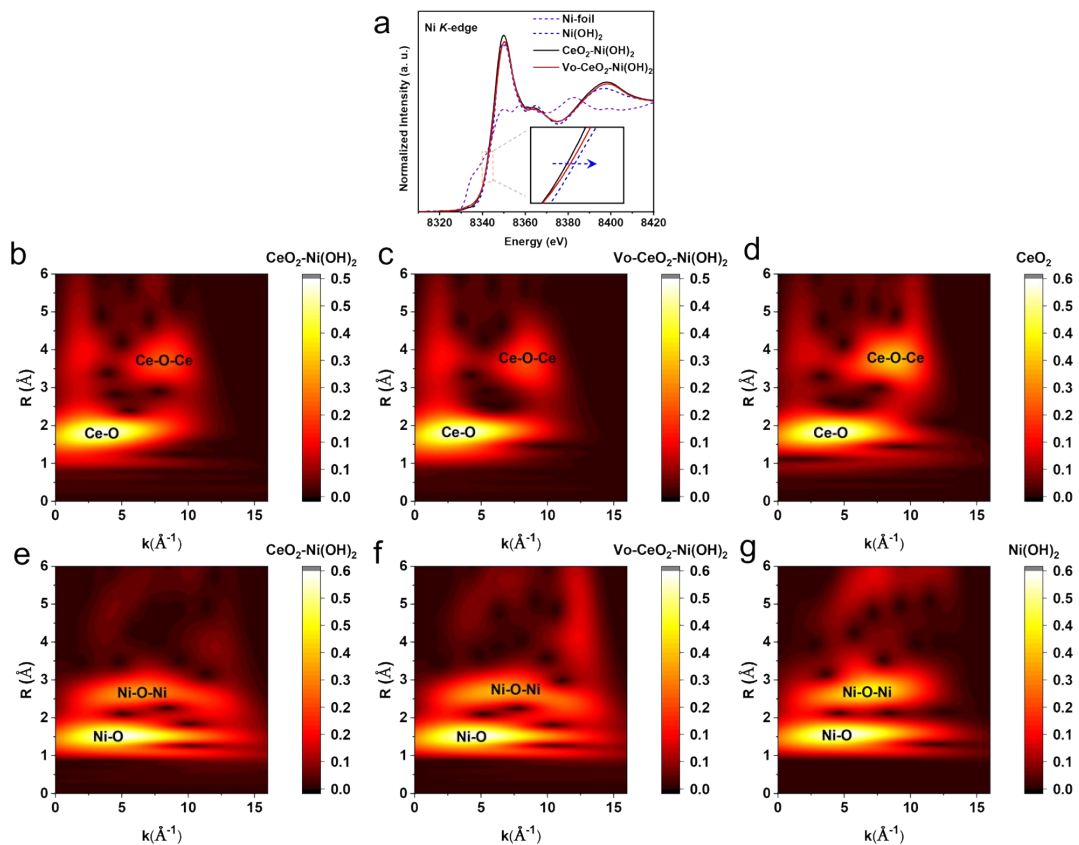


**Fig. S4** Characterization of the atomic coordination environment of  $V_0$ -CeO<sub>2</sub>-Ni(OH)<sub>2</sub> and CeO<sub>2</sub>-Ni(OH)<sub>2</sub>. (a) Ni *K*-edge XANES spectra of the samples, the inset shows a magnified view of the absorption edge. (b-d) Wavelet transform (WT) contour plots of the Ce *L*-edge EXAFS for (b) CeO<sub>2</sub>-Ni(OH)<sub>2</sub>, (c)  $V_0$ -CeO<sub>2</sub>-Ni(OH)<sub>2</sub>, and (d) CeO<sub>2</sub> samples. (e-g) Wavelet transform (WT) contour plots of the Ni *K*-edge EXAFS for (e) CeO<sub>2</sub>-Ni(OH)<sub>2</sub>, (f)  $V_0$ -CeO<sub>2</sub>-Ni(OH)<sub>2</sub>, and (g) Ni(OH)<sub>2</sub> samples.

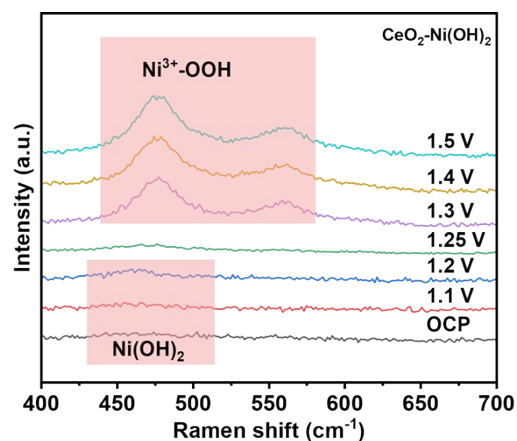


**Fig. S5** In situ Raman spectra of  $\text{CeO}_2\text{-Ni(OH)}_2$  in 1 M KOH with 300 mM 1,5-PDO over a potential range from open circuit potential (OCP) to 1.5 V (vs. RHE).

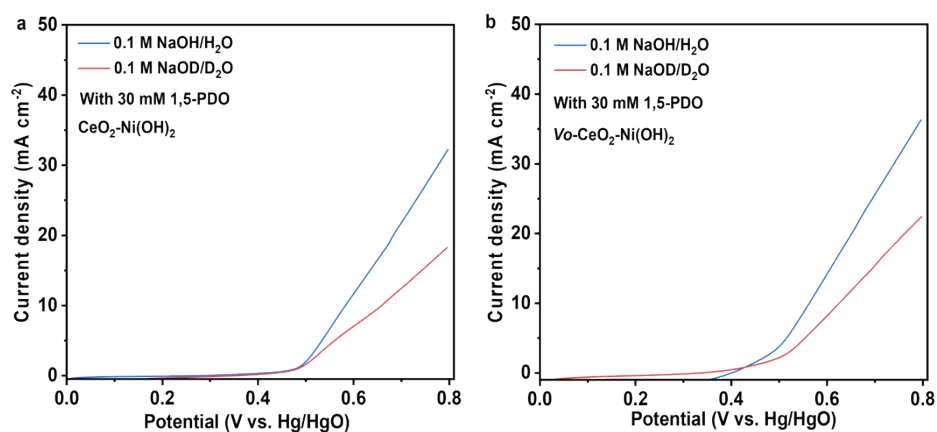


**Fig. S6** . LSV curves of (a)  $\text{CeO}_2\text{-Ni(OH)}_2$  and (b)  $\text{Vo-CeO}_2\text{-Ni(OH)}_2$  in 0.1 M OH-/H<sub>2</sub>O and 0.1 M OD-/D<sub>2</sub>O in the presence of 30 mM 1,5-pentanediol, respectively.

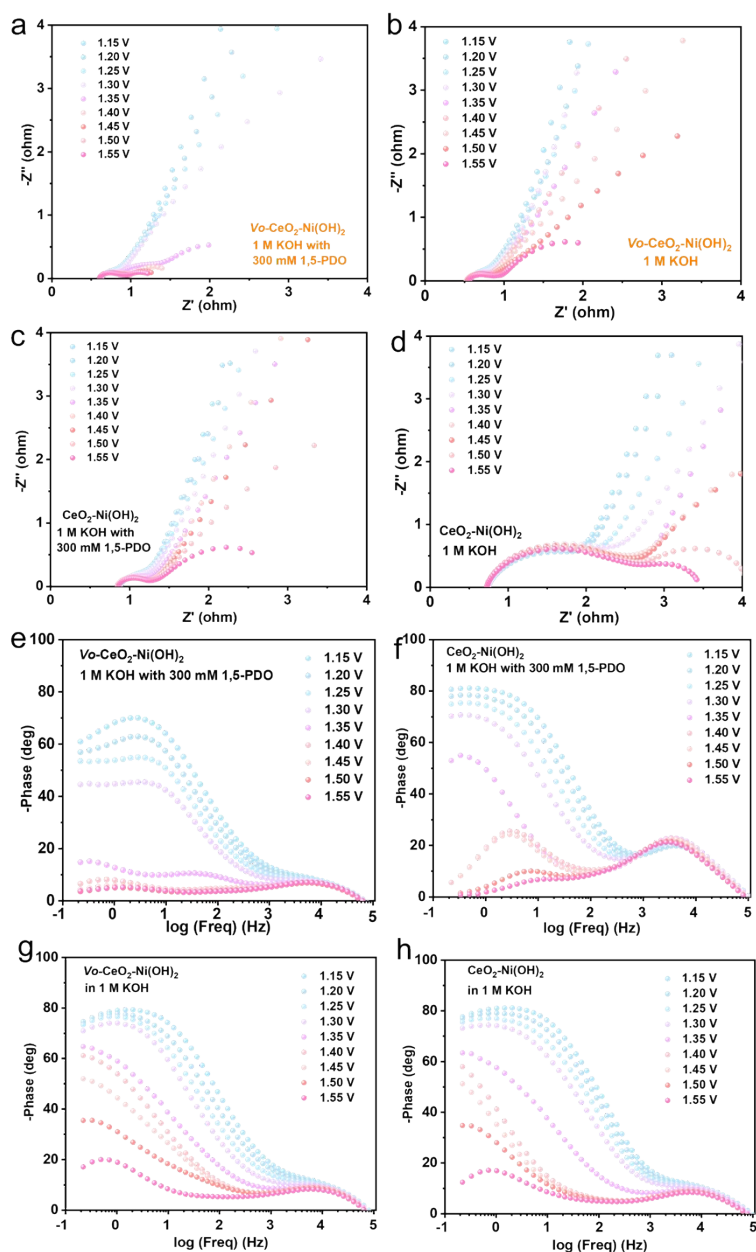


**Fig. S7** Detailed EIS of the  $V\text{o-CeO}_2\text{-Ni(OH)}_2$  and  $\text{CeO}_2\text{-Ni(OH)}_2$  under different potentials and electrolyte environments. (a, b) Nyquist plots of  $V\text{o-CeO}_2\text{-Ni(OH)}_2$  in (a) 1 M KOH with 300 mM 1,5-PDO and (b) 1 M KOH. (c, d) Nyquist plots of  $\text{CeO}_2\text{-Ni(OH)}_2$  in (c) 1 M KOH with 300 mM 1,5-PDO and (d) 1 M KOH electrolyte. (e-h) EIS Bode phase angle plots under different catalysts and electrolyte systems: (e)  $V\text{o-CeO}_2\text{-Ni(OH)}_2$  in 1 M KOH with 1,5-PDO, (f)  $\text{CeO}_2\text{-Ni(OH)}_2$  in 1 M KOH with 1,5-PDO, (g)  $V\text{o-CeO}_2\text{-Ni(OH)}_2$  in 1 M KOH, (h) Bode phase angle plots of  $\text{CeO}_2\text{-Ni(OH)}_2$  in 1 M KOH electrolyte. All measurements were performed within the potential range of 1.15 V to 1.55 V (vs. RHE).

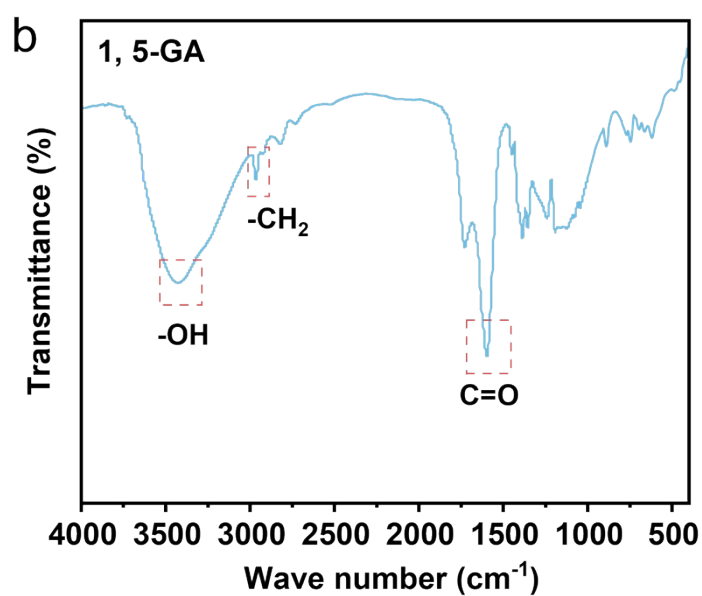
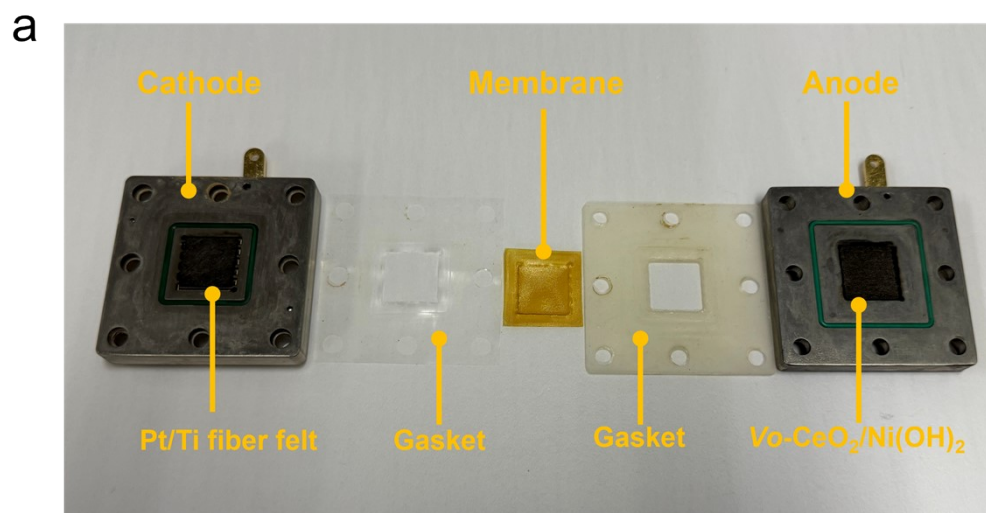


**Fig. S8** Photograph of the MEA system components (a) and the FT-IR spectrum of the product 1,5-GA (b). Characteristic peaks are shown for -OH (approximately 3400 cm<sup>-1</sup>), -CH<sub>2</sub>- (approximately 2950 cm<sup>-1</sup>), and the typical C=O (approximately 1700 cm<sup>-1</sup>) of the carboxyl group.